

## Heavy-ion physics with the ALICE detector

D. MIŚKOWIEC ON BEHALF OF THE ALICE COLLABORATION

*GSI Helmholtzzentrum für Schwerionenforschung GmbH, Darmstadt, Germany*

**Summary.** — A selection of recent results from the heavy-ion experiment ALICE at the CERN LHC, chosen to address various stages of the nucleus-nucleus reaction.

### 1. – Introduction

It is CERN's mission to “unite people from all over the world (...) for the benefit of all.” The ALICE collaboration at CERN counts 2000 members from 40 countries studying the mechanism of collisions of lead nuclei at LHC energies and the properties of the special state of matter created therein. The ALICE apparatus and its performance are described in Refs. [1] and [2], respectively. Its main components are shown in Fig. 1. The

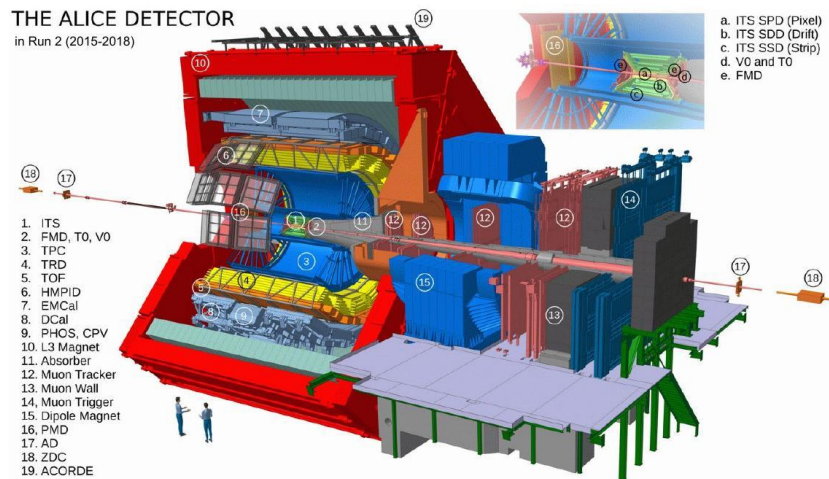


Fig. 1. – ALICE at the LHC. The central barrel detectors in a solenoid magnet cover midrapidity, forward muons are measured after an absorber and a dipole magnet, auxiliary detectors provide triggering and centrality determination.

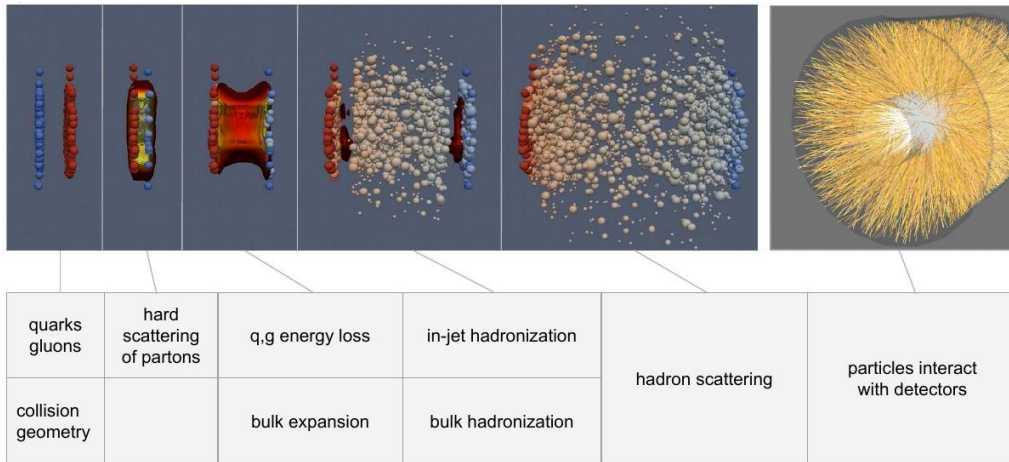


Fig. 2. – Main stages of a Pb–Pb collision at the LHC. See text. Visualization figure taken from Ref. [3].

central barrel detectors provide tracking and particle identification of charged particles within  $-0.9 < \eta < 0.9$  and electromagnetic calorimetry within  $-0.7 < \eta < 0.7$ . This is complemented by a muon detector at  $-4.0 < \eta < -2.5$  as well as several detectors for triggering and centrality determination.

The main stages of a Pb–Pb collision at the LHC are schematically represented in Fig. 2. The initial state depends on the collision centrality and on the distribution of nucleons within the colliding nuclei in the transverse plane. The nuclei, contracted by a Lorentz factor of  $\sim 2000$ , fly through each other and the space between their receding disks is filled with energy in form of gluons and quarks (quark-gluon plasma). It is helpful, in particular for non-central collision, to talk about collisions between pairs of nucleons [4]. The temporal sequence of these collisions does not depend on their longitudinal positions within nuclei. Instead, all nucleon-nucleon (NN) collisions are initiated at the same time and their duration depends on their hardness. Hard collisions finish first and get all the energy they want; this is why they scale with the number of NN collisions  $N_{\text{coll}}$ . Soft collisions take longer and compete among themselves for energy, so they scale like the total available energy or the number of participating nucleons,  $N_{\text{part}}$ . Hard collisions do not compete against soft collisions because they are faster, and do not compete among themselves because they are rare.

Heavy quarks and high- $p_T$  quarks and gluons are produced in hard processes. The ones with a larger than average transverse velocity have to traverse a portion of the elongated fireball in the transverse direction. They scatter and radiate, equilibrating their transverse velocity with the surrounding medium. By measuring their energy loss one learns about the properties of the quark-gluon plasma.

The fireball keeps expanding until the energy density drops below  $1 \text{ GeV}/\text{fm}^3$ , at which point the quarks and gluons have to form color neutral hadrons. This process turns out to depend on the environment. The formed hadrons interact with each other inelastically, then only elastically. The chemical and kinetic freeze-out mark the ends of these two phases and shape the hadron yields and momenta, respectively. Finally, the hadrons propagate freely until they interact with our detectors.

In this talk I am briefly discussing several recent (less than 1 year old) ALICE results, which uniformly address all stages of the nuclear collisions at the LHC. The reader is referred to the respective ALICE publications for details.

## 2. – Initial state: Correlation between the elliptic flow and the mean transverse momentum

Initial conditions, namely the collision centrality and the transverse distributions of nucleons within the colliding nuclei, define the transverse energy density profile of the collision system. The average transverse momentum of emerging particles and the Fourier coefficients of their azimuthal distribution fluctuate event by event. Since both depend on the initial conditions, it is interesting to look for a correlation between them. It turns out [5] that the second Fourier coefficient  $v_2$  of the azimuthal distribution of particles is positively correlated with the average  $p_T$  for all centralities between zero and 60% (Fig. 3). Following conclusions can be reached by comparing the measurement with several hydro

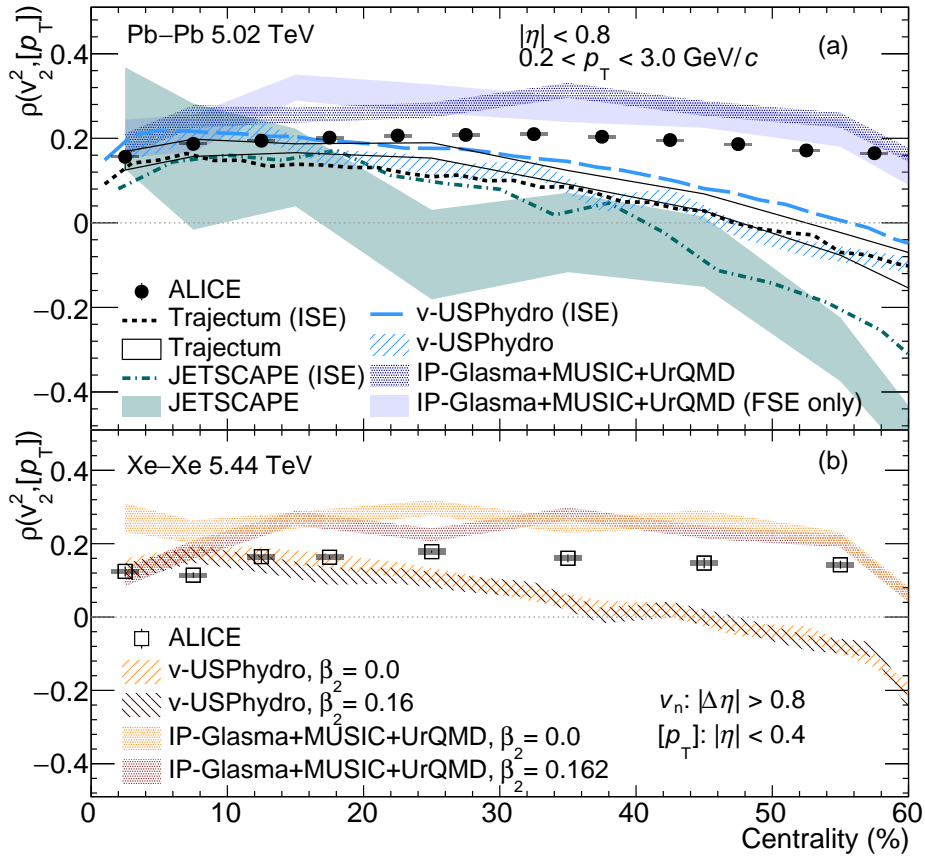


Fig. 3. – Correlation between the elliptic flow (azimuthal anisotropy of particle emission) and the mean transverse momentum of charged particles in Pb-Pb and Xe-Xe collisions [5]. Models using the Color Glass Condensate approach describe the measurement better than those based on T<sub>R</sub>ENTo.

models: i) the correlation coefficient is indeed sensitive to the initial conditions, ii) it is only weakly affected by the subsequent stages, and iii) its magnitude and centrality dependence are described by models based on IP-Glasma better than those based on T<sub>R</sub>ENTo. The second statement is supported by the proximity of analytic initial-state estimations (ISE, lines) to the respective full hydrodynamic calculations (shaded areas). IP-Glasma is the Color Glass Condensate effective theory in which the initial conditions are dominated by the distribution of gluons. This is different from T<sub>R</sub>ENTo based models, in which the dominant degrees of freedom are those of nucleons. Understanding the initial conditions is a prerequisite for the study of quark-gluon plasma.

### 3. – Hard processes: beauty production

Heavy-flavor quarks  $c$  and  $b$  decay weakly into lighter flavors. As seen by the values of the CKM matrix elements, their most favored decays are  $b \rightarrow c$  and  $c \rightarrow s$ . A special case of  $b$  decay with two flavor changing vertices is its decay into  $J/\psi$  (Fig. 4 left). Weak decays of  $s$ ,  $c$ , and  $b$  quarks result in characteristic hadron lifetimes of  $c\tau \sim 2\text{-}400$  cm,  $0.1\text{-}0.3$  mm, and  $0.4\text{-}0.5$  mm, respectively. A measurement of non-prompt (i.e. those not originating from the primary collision vertex)  $J/\psi$  can thus be used to determine the yield of beauty hadrons. The cross section of midrapidity beauty production in  $pp$  collisions at several LHC energies, deduced from recent ALICE measurement of non-prompt  $J/\psi$ , is shown in Fig. 4 right [6]. The ALICE points match the overall collision energy systematics and improve its precision. The  $J/\psi$  mesons were measured in the  $J/\psi \rightarrow e^+e^-$  decay channel. The good vertexing performance of ALICE central barrel allowed for an efficient selection of non-prompt  $J/\psi$ . The relation between the non-prompt  $J/\psi$  yield and the  $b$  production cross section was taken from state-of-the-art models. This analysis complements the ALICE measurements of beauty via non-prompt  $D$  and  $\Lambda_c$ .

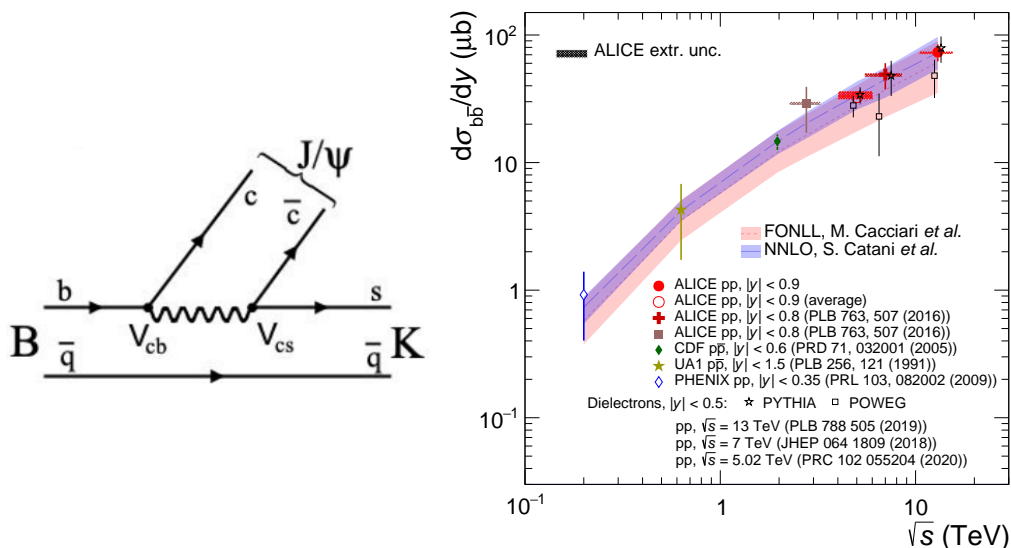


Fig. 4. – Left: Beauty decay into non-prompt  $J/\psi$  (figure taken from Ref.[7]). Right: Collision energy dependence of the beauty production cross section at midrapidity [6].

#### 4. – Energy loss of c quarks

Hard parton scatterings in the early stage of the Pb–Pb collision are the main source of quarks with high mass and/or transverse momentum. Those quarks that are moving transversally outwards faster than average will lose part of their energy by interacting with the – slowly expanding – soft partonic bulk. Assuming that the emerging hadrons have a similar velocity as their constituent quarks before hadronization, the experimental signature should be a reduction of the high- $p_T$  yield in central Pb–Pb collisions compared to pp. The characteristic  $p_T$  above which this suppression occurs should depend on the quark mass. Figure 5 shows the nuclear modification factor  $R_{AA}$ , defined as the ratio of the transverse-momentum spectrum measured in Pb–Pb collisions of a given centrality, divided by the mean number of nucleon-nucleon collisions  $N_{\text{coll}}$ , to the one measured in pp. Values below unity indicate energy loss. The ALICE measurement of  $D^0$  (black points in Fig. 5) demonstrates that charm quarks interact with medium and lose energy [8]. The detailed shape of the  $p_T$  dependence systematically changes with the hadron (or its heaviest quark) mass.

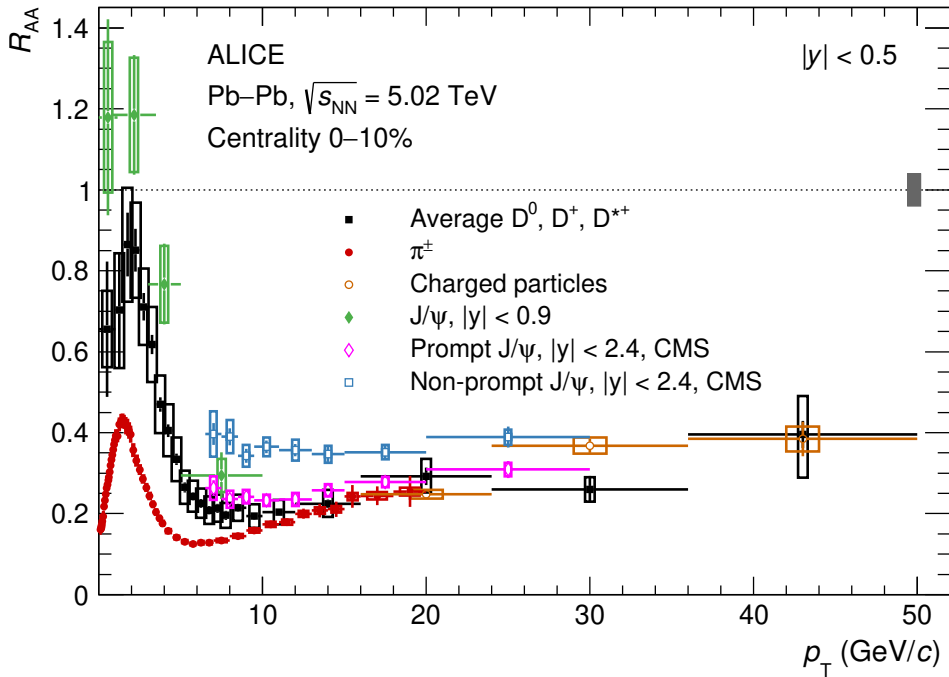


Fig. 5. – Nuclear modification factor of the  $D^0$  yield (black points) compared to several other hadron species. The  $D^0$  measurement reaches down to  $p_T = 0$  [8].

Light and heavy hadron species get united in the limit of high  $p_T$ , except for the non-prompt  $J/\psi$  – a proxy for beauty – which for  $p_T = 10$ – $20$   $\text{GeV}/c$  seems to lie somewhat higher than the rest. This suggests that b quarks at these transverse momenta lose less energy than c quarks [8, 9]. The quark energy loss in this region is dominated by the radiation of gluons. A probable reason for a reduction of the radiative energy loss of the b quark is discussed in Section 5.

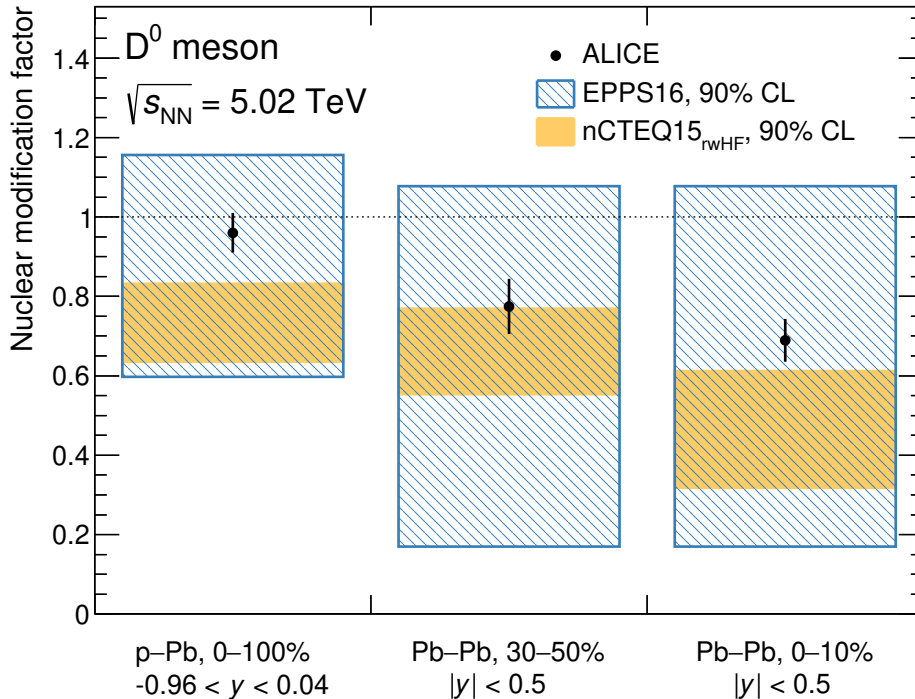


Fig. 6. – The  $p_T$ -integrated nuclear modification factor of the  $D^0$  yield in Pb–Pb collisions. The total number of  $D^0$  is not as strongly suppressed as the high- $p_T$  part of its spectrum.

Strictly speaking, energy loss should lead to a shift to lower  $p_T$  rather than disappearance. Since the  $D^0$  has been measured down to  $p_T = 0$ , one can integrate the spectrum and compare the total yields in Pb–Pb and pp collisions. This is shown in Fig. 6. The  $p_T$ -integrated suppression of  $D^0$  in Pb–Pb is two times weaker than the suppression of the high- $p_T$  part of their spectrum. This overall suppression may come from the initial stage: a reduced production of  $c$  quarks resulting from modifications of the parton distribution function in Pb (shadowing). Alternatively it can have to do with the late stage, namely with enhanced hadronization of the  $c$  quark into hadrons other than  $D^0$ . This will be discussed in Section 6.

### 5. – Energy loss of $b$ quarks: dead cone

Radiation of gluons by quarks, no matter whether in a colored medium or in vacuum, is restricted to polar angles larger than  $m/E$  of the radiating quark (dead-cone effect). A detailed investigation of this phenomenon has been performed by ALICE in pp collisions using jets containing a  $D^0$ , and resulted in the first direct experimental observation of the dead cone [10]. The  $D^0$  mesons were reconstructed in the  $D^0 \rightarrow K^- \pi^+$  channel. Assuming that the  $c$  quark of  $D^0$  was the leading quark of the jet, one can reconstruct the complete history of the splittings which lead to the jet. For this, one assumes that the  $c$  quark energy (obviously) and the splitting angle (because of the angular ordering)

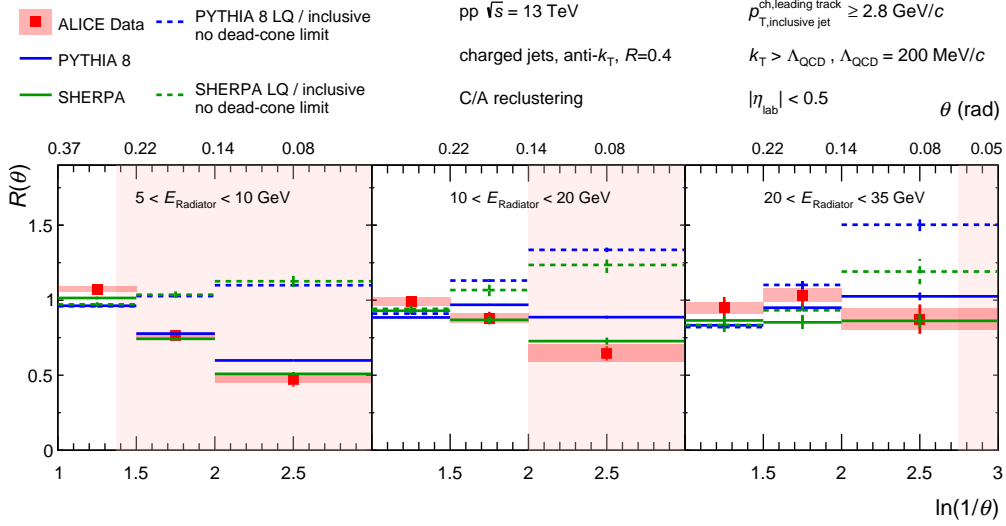


Fig. 7. – The dead cone effect in the radiative energy loss of  $c$  quark in pp collisions, visible as a reduction of small-angle splittings [10].

decrease during the fragmentation. The distribution of the splitting angles in  $D^0$  jets, divided by the analogous distribution in light-flavor jets, is shown in Fig. 7. The number of small-angle splittings in jets initiated by  $c$  quarks with  $5 < E_{\text{Radiator}} < 10$  GeV (third bin in the leftmost panel) is two times lower than in light-flavor jets. The suppression of small-angle splittings gradually disappears when going to higher quark energies (the two right panels).

## 6. – Hadronization in medium

Heavy quarks ( $c$ ,  $b$ ) are created in hard parton scatterings at the beginning of the nucleus–nucleus collision and their total number is conserved in the subsequent stages. Subject to scattering in medium, they suffer energy loss and partially adapt their velocities to the surrounding bulk, thus – to some degree – participating in its collective motion. At the end of the partonic phase they hadronize and emerge from the reaction as heavy mesons and baryons. Their detailed distribution over various hadron species (fragmentation fractions) is important to know because not always one can afford measuring all of them to get a complete picture. The fragmentation fractions are not universal, as one can see already when comparing the charmed particles emerging from  $ee$  and  $pp$  collisions. This is shown in Fig. 8, in which the ALICE points represent the first measurement of charm fragmentation fractions at the LHC and the first measurement ever of the  $c$  fragmentation fraction to  $\Xi_c$  [11]. Compared to  $ee$  and  $ep$ , in  $pp$  collisions a clear increase of the  $\Lambda_c^+$  fraction and decrease of  $D^0$  are seen. This means that hadronization depends on the environment. Models including the hadronization via coalescence with surrounding quarks are able to describe the data. A further gradual increase of  $\Lambda_c^+/D^0$  is visible when going from  $pp$  to semicentral and to central Pb–Pb collisions [12].

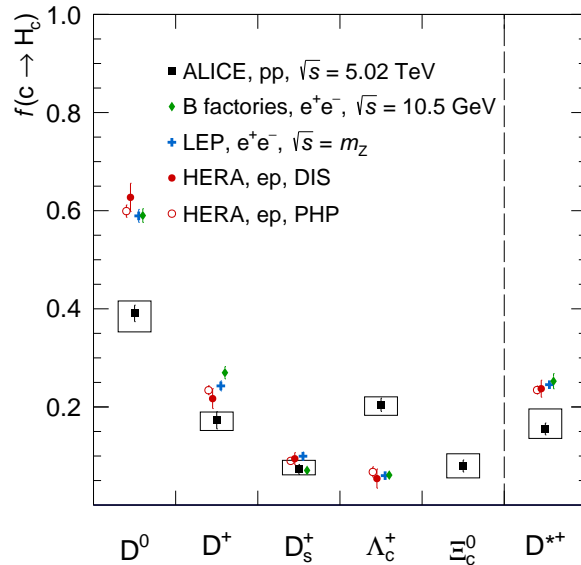


Fig. 8. – Charm hadronization in high energy ee, ep, and pp collisions [11]. The charmed baryons are significantly enhanced in pp as compared to ee and ep collision systems.

## 7. – Closing remarks

ALICE used its strengths – low- $p_T$  tracking, particle identification, vertexing – not only to study in detail various stages of Pb–Pb collisions but also to understand the elementary QCD phenomena without which the interpretation of the Pb–Pb data would not be possible. This activity will be continued in the just starting (in June 2022) Run 3 of the LHC, for which significant upgrades of the ALICE detectors and readout were performed in the Long Shutdown 2.

\* \* \*

The author thanks the organizers for inviting ALICE to present its results. I acknowledge the creative and inspiring atmosphere and the nice settings of the conference.

## REFERENCES

- [1] K. Aamodt *et al.* [ALICE], JINST **3** (2008), S08002 doi:10.1088/1748-0221/3/08/S08002.
- [2] B. B. Abelev *et al.* [ALICE], Int. J. Mod. Phys. A **29** (2014), 1430044.
- [3] MADAI collaboration, Hannah Petersen and Jonah Bernhard.
- [4] A Białas, M Bleszyński, and W Czyż, Nucl. Phys. B 111(1976)461.
- [5] S. Acharya *et al.* [ALICE], [arXiv:2111.06106 [nucl-ex]].
- [6] S. Acharya *et al.* [ALICE], JHEP **03** (2022), 190.
- [7] Norbert Neumeister, DELPHI, Ph.D. thesis, 1996.
- [8] S. Acharya *et al.* [ALICE], JHEP **01** (2022), 174.
- [9] S. Acharya *et al.* [ALICE], [arXiv:2202.00815 [nucl-ex]].
- [10] S. Acharya *et al.* [ALICE], Nature **605** (2022) no.7910, 440-446.
- [11] S. Acharya *et al.* [ALICE], Phys. Rev. D **105** (2022) no.1, L011103.
- [12] S. Acharya *et al.* [ALICE], [arXiv:2112.08156 [nucl-ex]].